



Available online at www.sciencedirect.com

SCIENCE @ DIRECT®

C. R. Mecanique 332 (2004) 345–351



Microgravity and Transfer/Critical fluids

Thermoconvective instabilities in supercritical fluids

Sakir Amiroudine ^{a,*}, Bernard Zappoli ^b

^a ENSAM, EMT/LPMI, 2, boulevard du Ronceray, BP 93525, 49035 Angers, France

^b CNES, 18, avenue Ed. Belin, 31000 Toulouse, France

Available online 21 April 2004

Abstract

A numerical solution of the Navier–Stokes equations coupled with the energy and linearised equation of state has been performed in the unsteady Rayleigh–Bénard configuration for nearly supercritical ³He in the exact conditions with which Meyer and Kogan (Phys. Rev. E 63 (2002) 056310) performed their experiments. We propose an interpretation of the observed unexpected temperature oscillations at the convection onset in terms of coupled hot and cold piston effects. We have also considered the stability of two layers (hot and cold) of a same supercritical fluid in an unstable configuration. The first results show an analogy between the diffusion of species (Rayleigh–Taylor like instability) and thermal diffusion considered in this study. **To cite this article:** S. Amiroudine, B. Zappoli, C. R. Mecanique 332 (2004).

© 2004 Académie des sciences. Published by Elsevier SAS. All rights reserved.

Résumé

Instabilités thermoconvectives dans les fluides supercritiques. La première partie de l'article concerne la convection de Rayleigh–Bénard instationnaire dans de l'³He supercritique telle qu'elle apparaît dans les conditions expérimentales de Meyer et Kogan (Phys. Rev. E 63 (2002) 056310). Cette étude est menée en résolvant numériquement les équations de Navier–Stokes couplées avec l'équation d'état linéarisée et celle de l'énergie. Les oscillations temporelles inattendues de la température ont été interprétées en terme de compétition entre les effets piston chaud et froid. Dans un deuxième temps, nous avons considéré la stabilité de deux couches superposées, chaude et froide d'un même fluide supercritique isobare en configuration instable. Les premiers résultats confortent bien l'idée de l'analogie entre la diffusion des espèces (instabilité de Rayleigh–Taylor) et la diffusion thermique considérée dans cette étude. **Pour citer cet article :** S. Amiroudine, B. Zappoli, C. R. Mecanique 332 (2004).

© 2004 Académie des sciences. Published by Elsevier SAS. All rights reserved.

Keywords: Supercritical fluid; Piston effect; Instability; Finite volume

Mots-clés : Fluide supercritique ; Effet piston ; Instabilité

* Corresponding author.

E-mail address: Sakir.amiroudine@angers.ensam.fr (S. Amiroudine).

1. Introduction

The hydrodynamic stability of the steady heat conduction and incompressible or moderately compressible fluid layer is a classical problem, which obeys the Rayleigh criterion. For a compressible fluid and for fluid columns of large dimensions, the criterion based on the adiabatic temperature gradient (ATG) replaces the Rayleigh criterion for the onset of convection [1–4]. The effects associated with the ATG (well known in atmospheric sciences) have not been studied in controlled laboratory experiments. As the compressibility diverges at the critical point (CP), the transition curve for the onset of convection has been shown experimentally [1], analytically [3] and numerically [2,4], to display a crossover from a Rayleigh-dominated regime to one determined by the ATG.

In the recent experiments of Meyer and Kogan [1], temporal oscillations in the temperature field were observed above the onset of convection in a Rayleigh–Bénard cell filled with supercritical ^3He . The fluid, which was contained in a cylindrical cell of large aspect ratio, is heated from below by a constant flux and the upper plate is maintained at the initial temperature. Numerical simulations by different groups [4,5] have also characterized these oscillations by using different methods. We explain here with the help of Navier–Stokes numerical simulations that the cold piston effect (CPE, see [6] for details) initiated by the thermal plumes is responsible for the observed temperature oscillations.

In continuity with the above study which is characterized by the unstable upper layer caused by the CPE, we have considered the simulation of the stability of two superposed layers, hot and cold of the same supercritical pure fluid, which are placed in an unstable configuration. The analysis of the growth rate of the instability for different wave numbers shows the existence of a cut-off wavenumber above which small wavelengths are stabilized. The agreement between the numerical values and recent theories on the stability of a diffusion front of miscible fluids confirms that a pure supercritical fluid, which presents a thermal gradient, may lead to the development of a gravitational instability. The density gradient (as in Rayleigh–Taylor instabilities) is not determined by the diffusion of species but by thermal diffusion and high compressibility [7]. The results are given as a function of the proximity to CP in order to establish stability diagrams of two superposed layers of a pure supercritical fluid.

2. Model

We consider a 2D rectangular cavity (2 mm long and 1 mm high), which is heated from below by a constant heat flux with periodic boundary conditions on the lateral walls in order to correctly represent the large aspect ratio ($\cong 50$) in the experiment of Meyer and Kogan [1]. The upper wall is maintained at a fixed temperature $T_0 = (1 + \varepsilon)T_c$, where T_c is the critical temperature and ε represents the distance to the critical point. The cavity, filled with supercritical ^3He , is initially at the critical density (ρ_c). All the thermophysical properties correspond to the experimental data [1]. In addition to the Navier–Stokes equations corresponding to the motion of the fluid in the cavity, we consider the equation of energy and the linearised equation of state:

$$\begin{aligned} \rho C_p \frac{dT}{dt} &= T \beta_P \frac{\partial P}{\partial t} + \nabla(\lambda \nabla T) + \Phi; & \text{Energy} \\ \rho &= \rho_0 + \rho_c \chi_T (P - P_0) - \rho_c \beta_P (T - T_0); & \text{State} \end{aligned}$$

where β_P is the thermal expansion coefficient, χ_T the isothermal compressibility, λ the thermal conductivity, C_p the specific heat at constant pressure, $\Phi = \sigma_{ij} \partial V_i / \partial x_j$ the dissipation function with σ_{ij} the stress tensor, V_i the velocity components, P_0 and T_0 the initial pressure and temperature fields.

The above equations are solved numerically by the finite volume method using the SIMPLER algorithm [2]. The discretisation is 1st order Euler in time and uses the power-law scheme of Patankar [8] in space. A non-uniform mesh in a staggered grid has been used and numerical stability in terms of time-step and mesh size has been carefully checked. All the interesting physical phenomena being on a longer time scale (i.e. the piston-effect time scale, see [2] for details) than the acoustic time scale, an acoustic filtering procedure has been included in the

numerical code. This implies: (i) a reduction of computer time because of higher time steps; and (ii) a dependence of pressure in time determined by mass conservation.

3. Thermal oscillations at the Rayleigh–Bénard threshold in supercritical ³He

For a compressible fluid with large dimensions of the cavity or a highly compressible fluid in the laboratory, the stabilized adiabatic temperature gradient $ATG \equiv (-g\rho/\beta_P)(\chi_T - \chi_S) = -gT_c\beta_P/C_p$, modifies the usual definition of the Rayleigh number for the onset of convection (here χ_S is the isentropic compressibility and g the gravity). It is given by [9]: $Ra^{new} = Ra(1 - ATG \cdot L/\Delta T) \geq Ra_c (\cong 1708)$. We have run simulations based on the experimental data [1] ($\kappa = 10^{-9}$ m²/s, $C_p = 5.18 \times 10^5$ J/kg/K, $\chi_T = 4.3 \times 10^{-4}$ Pa⁻¹, $\beta = 52$ K⁻¹ and the critical values: $T_c = 3.318$ K, $\rho_c = 41.4$ kg/m³ and $P_c = 1.17$ bar) with $\varepsilon = 0.01$ and for different heat fluxes. Fig. 1(a) shows the temperature field at the steady state as a function of heat flux and for different values of Ra^{new} . The numerical results agree well with the experimental ones, which is confirmed by the time evolution of the temperature field (Fig. 1(b)) for a heat flux of 4.7×10^{-3} W/m². The maximum error is of the order of 22% and a good synchronization is obtained for the oscillations. This case corresponds to the damped oscillations in the instability diagram established by Meyer and Kogan [1], as in Fig. 2 for a heat flux of 6.65×10^{-4} W/m². It constitutes the basis for our interpretation of these oscillations.

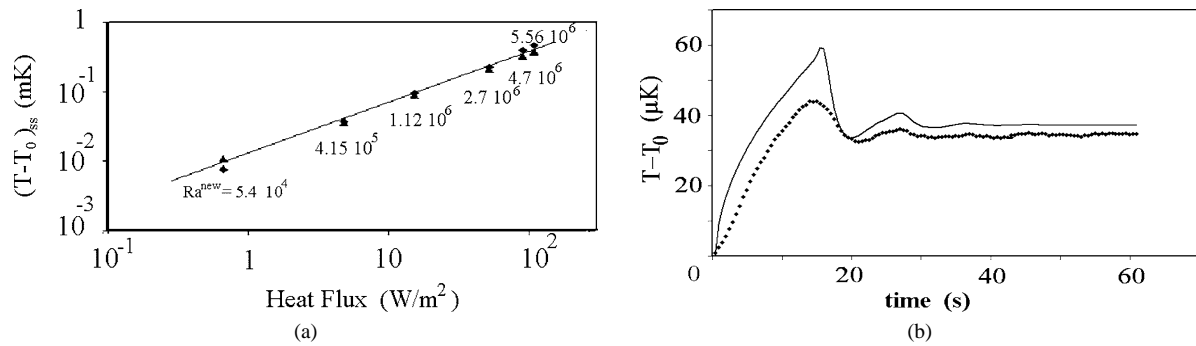


Fig. 1. (a) Comparison in a log-log scale between experimental (▲) [1] and numerical results (◆) of the steady state (ss) temperature as a function of heat flux for $\varepsilon = 0.01$. (b) Experimental (◆) and numerical (solid line) temperature fields as a function of time at the lower plate for a heat flux of 4.78×10^{-3} W/m².

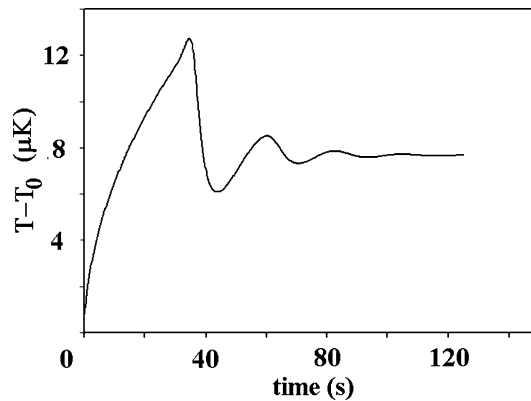


Fig. 2. Numerical temperature field as a function of time on the bottom layer for a heat flux of 6.65×10^{-4} W/m².

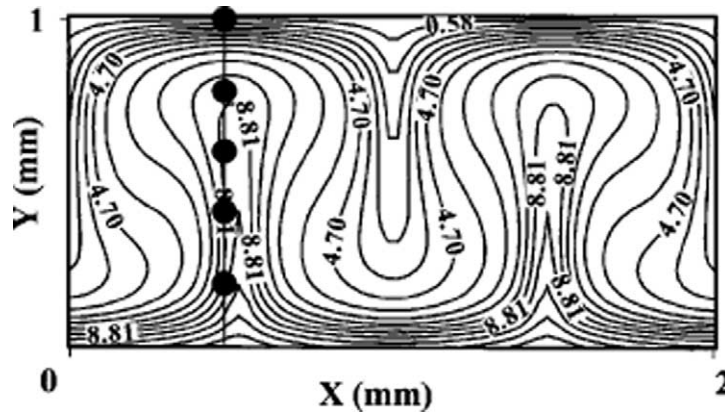


Fig. 3. Temperature field $[(T - T_0) \mu\text{K}]$ at $t = 36$ s for a heat flux of $6.65 \times 10^{-4} \text{ W/m}^2$. The different points correspond to the localization of the temporal evolution of the temperature field on Fig. 4.

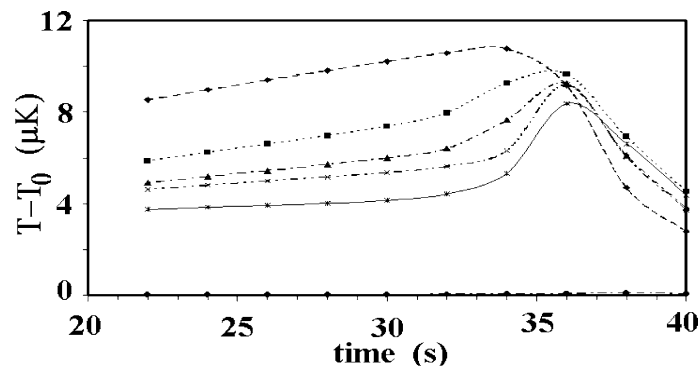


Fig. 4. Temperature differences as a function of time for different heights and a heat flux of $6.65 \times 10^{-4} \text{ W/m}^2$: (-♦-: $x = 0.25$ mm, $y = 0.5$ mm, -■-: $x = 0.5$ mm, $y = 0.2$ mm, -▲-: $x = 0.5$ mm, $y = 0.4$ mm, -×-: $x = 0.5$ mm, $y = 0.6$ mm, -*: $x = 0.5$ mm, $y = 0.8$ mm, -●-: $x = 0.5$ mm, $y = 1$ mm).

Two diffusive boundary layers form on the top and bottom plates of the cavity after the beginning of heating. A competition between the two piston effects exists during this diffusive period until the beginning of convection with the appearance of thermal plumes. Fig. 3 shows the temperature field at $t = 36$ s and different points where the temperature is numerically evaluated for a heat flux of $6.65 \times 10^{-4} \text{ W/m}^2$ and Fig. 4 represents the time evolution of the temperature field for these different heights at $x = 0.5$ mm. At $y \cong 0.8$ mm, the change of slope at $t = 32$ s corresponds to the beginning of convection; then at $t = 34$ s, another change of slope is seen at this same location corresponding to the incoming of hot fluid by the thermal plume. This increase of temperature gradient provokes an increase of the CPE [6], which involves a homogeneous decrease of the temperature in the bulk even if the latter always brings hot fluid from the bottom plate. This homogeneous decrease of the temperature is the signature of the piston effect. The temperature of the bottom plate has thus to decrease because the heat flux is imposed on that plate. Two antagonistic effects take place: an increase of the temperature due to convection and decrease corresponding to the piston effect.

Fig. 5 shows the temperature at $x = 0.5$ mm as a function of the vertical position. We can notice a typical piston effect profile between 22 s and 32 s in the diffusive regime, then two convective profiles ($t = 36$ s, $t = 38$ s). The temperature gradient at $y = 1$ becomes more and more important and reaches a maximum at $t = 38$ s. Between 38 s and 40 s, we note a sharp decrease of the temperature in the bulk which involves a decrease of the temperature

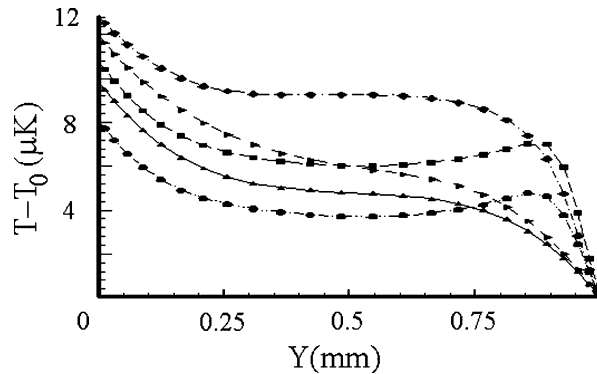


Fig. 5. Vertical temperature profiles at $x = 0.5$ mm and at different times for a heat flux of 6.65×10^{-4} W/m². (—▲—: $t = 22$ s, --■--: $t = 32$ s, ···◆···: $t = 36$ s, -·-■-·: $t = 38$ s, -·-●-·-·: $t = 40$ s).

of the bottom plate where the heat flux is fixed. Fig. 4 shows also the evolution of the temperature at $x = 0.25$ mm, $y = 0.5$ mm, where the magnitude of the velocity field is very weak (3–4 $\mu\text{m/s}$, whereas it is of the order of 500 $\mu\text{m/s}$ in the center of the thermal plume), which proves also the absence of convection and confirms the signature of the piston effect. The decrease of the temperature in the bulk between 34 s and 40 s, with a maximum at 38 s, is due to the competition between the hot and cold piston effects because thermal diffusion is negligible. The oscillatory phenomenon is then simple to explain: when the temperature of the bulk decreases, the temperature gradient at the top plate decreases, involving a weakening of the cold piston effect. The hot piston effect then becomes dominant and a new ‘hot phase’ is initiated and the scenario described above reproduces with a damping.

4. Stability of two layers (hot and cold) placed in an unstable configuration

In the previous section, the diffusion layer along the upper plate, which is heavier than the fluid located just below it, gives birth to drips (Fig. 3) through a gravitational instability evocative of a Rayleigh–Taylor mechanism. The surface tension being a priori null (single-phase pure fluid), we have oriented our study towards a front diffusion instability, similar to that encountered in miscible fluids [10]. We have thus considered a simple situation in which an isobaric cavity of infinite extension is filled with a supercritical fluid, the top-half initial temperature of which is lower than that of the bottom-half. Periodic conditions at the lateral walls represent the infinite extension of the cavity as seen in the geometrical sketch of Fig. 6. Our main goal is to numerically study the stability of the thermal diffusion interface between the two halves of the cavity, via the analysis of the growth rate of the fluctuations. These fluctuations are simulated by the introduction of a sinusoidal initial perturbation of a field (for example the vertical velocity) at the interface: $v(x, y = 0.5, t = 0) = A \cos((2\pi/\tilde{\lambda})x)$, where A is the amplitude and $\tilde{\lambda}$ is the wavelength. The dynamical growth of the interface, i.e. the determination of the growth rate $\sigma(k)$, where $k(= 2\pi/\tilde{\lambda})$ is the wavenumber of the fluctuation introduced at $t = 0$, is deduced from the values of the vertical velocity at a point and at two times t_1 and t_2 with corresponding amplitudes A_1 and A_2 : $\sigma = \text{Ln}(A_1/A_2)/(t_1 - t_2)$.

We consider two initial reduced density differences ($(\rho_1 - \rho_2)/\rho_1 = 10^{-2}, 10^{-3}$) and we have used the experimental thermophysical properties of ³He [1]. The existence of a cut-off wavenumber above which small wavelengths are damped by diffusion is consistent with the conclusions of Kurowski et al. [10]. They have shown that the simultaneous effects of viscosity and diffusion is necessary for the existence of a cut-off wavelength given by: $\tilde{\lambda}_c = 2\pi(16\nu D/(3gR))^{1/3}$, where D is the interdiffusion coefficient in the case of miscible fluids (which is, by analogy in our case, the thermal diffusion coefficient), g is gravity and $R = (\rho_1 - \rho_2)/(\rho_1 + \rho_2)$ measures the

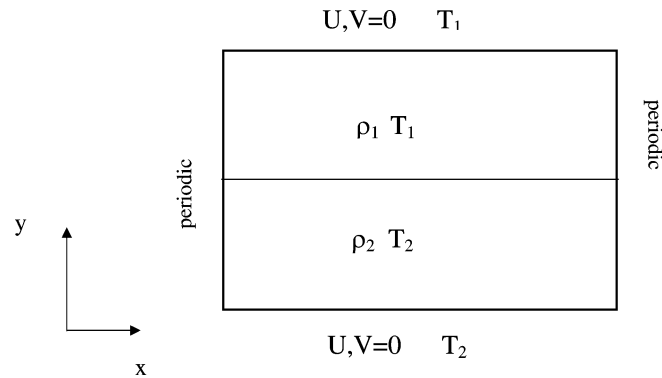
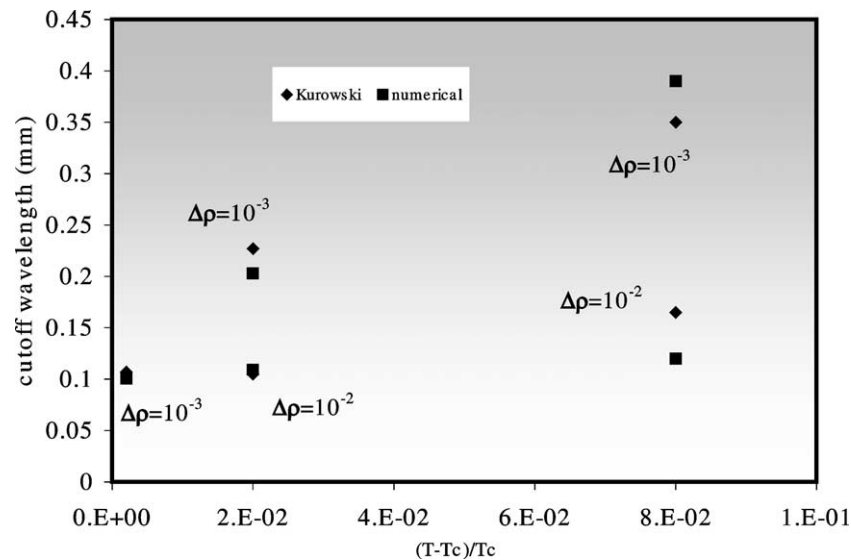


Fig. 6. Geometry of the 2D model.

Fig. 7. Theoretical and numerical cut-off wavenumbers as a function of $(T - T_c)/T_c$ for different values of the density difference $\Delta\rho = (\rho_1 - \rho_2)/\rho_1$.

density difference. Fig. 7 shows a good agreement between the theoretical [10] and the numerical results, which allows to justify the analogy between miscible liquids and thermally non-homogeneous isobaric supercritical fluids.

The space scales of the micro-drops formed by the instability are weak and it thus appears that the process of homogenization of a critical fluid on the ground can comprise a phase of micro-mixture during which the micro-drops are formed. These are then homogenized on a temporal scale, which is thus much shorter than the time scale of diffusion on the typical dimension of the cavity.

5. Conclusions

These two studies show the unforeseen behaviour of supercritical fluids in terms of thermal instabilities. In the first configuration where the fluid is heated from below, the onset of Rayleigh–Bénard convection is accompanied by thermal oscillations which can be explained by the interaction of the cold piston effect initiated at the upper

isothermal wall by the convective plume and the hot piston effect due to the heating of the lower wall. As for the second study, it shows that a pure supercritical fluid at two different temperatures can behave as two distinct fluids, miscible and the other. The current continuation of this work attempts to explore the stability conditions when the depth of the top-colder layer is very small compared the bottom hotter one.

Acknowledgements

This work has been supported by CNES (Centre National d'études Spatiales). The authors thank IDRIS, the Supercomputing Center (Orsay).

References

- [1] H. Meyer, A.B. Kogan, Onset of convection in a very compressible fluid: the transient toward steady state, *Phys. Rev. E* 63 (2002) 056310.
- [2] S. Amiroudine, P. Bontoux, P. Larroudé, B. Gilly, B. Zappoli, Direct numerical simulation of unsteady instabilities inside a near-critical fluid layer heated from below, *J. Fluid Mech.* 442 (2001) 119–140.
- [3] P. Carlès, B. Ugurtas, The onset of convection near the liquid–vapour critical point, Part I: Stationary initial state, *Physica D* 126 (1–2) (1999) 69–82.
- [4] Y. Chiwata, A. Onuki, Thermal plumes and convection in highly compressible fluids, *Phys. Rev. Lett.* 87 (2001) 144301.
- [5] S. Amiroudine, B. Zappoli, Piston effect induced thermal oscillations at the Rayleigh–Bénard threshold in supercritical ^3He , *Phys. Rev. Lett.* 90 (2003) 105303.
- [6] B. Zappoli, A. Jounet, S. Amiroudine, K. Mojtabi, Thermoacoustic heating and cooling in near-critical fluids in the presence of a thermal plume, *J. Fluid Mech.* 388 (1999) 389.
- [7] B. Zappoli, S. Amiroudine, S. Gauthier, Rayleigh–Taylor-like instability in near-critical pure fluids, *C. R. Acad. Sci. Paris, Sér. IIB* 324 (1997).
- [8] S. Patankar, *Numerical Heat Transfer and Fluid Flows*, MacGraw-Hill, 1980.
- [9] E.A. Spiegel, Convective instability in a compressible atmosphere, *Astrophys. J.* 141 (1965) 1068.
- [10] P. Kurowski, C. Misbah, S. Tchourkine, Gravitational instability of a fictitious front during mixing of miscible fluids, *Europhys. Lett.* 29 (4) (1995) 309–314.